Journal of Photochemistry and Photobiology A: Chemistry 211 (2010) 108–114

Contents lists available at ScienceDirect

Journal of Photochemistry and Photobiology A: Chemistry

journal homepage: www.elsevier.com/locate/jphotochem

Aggregation behaviour of a tetracarboxylic porphyrin in aqueous solution

Rita Giovannetti*, Leila Alibabaei, Laura Petetta

Section Chemistry of Environmental Science Department, Via S. Agostino, 1. University of Camerino (MC), 62032 Camerino, Italy

ARTICLE INFO

Article history:
Received 23 November 2009
Received in revised form 2 February 2010
Accepted 8 February 2010
Available online 13 February 2010

Keywords:
Coproporphyrin
Dimerization
Aggregation
Spectrophotometry
SEM

ABSTRACT

The aggregation of 3,8,13,18-tetramethyl-21H,23H-porphine-2,7,2,17-tetrapropionic acid (Coproporphyrin-I) has been investigated by UV–vis spectroscopy in aqueous solutions. The aggregation occurred by total neutralization of propionic groups and can be induced by alkaline salts, hydrogen peroxide or acidification. The hydrogen peroxide effect is investigated in the presence of different concentrations and it has been observed that only high concentrations favour the formation of H-aggregates. The dimerization constants in the several experimental conditions are reported. The *H-dimers* of Coproporphyrin-I in particular experimental conditions formed highly aggregate species depending on the pH. The kinetic of aggregation has been studied at different pHs and the results have showed that the log of kinetic constants k_P were linearly dependent on the pH. The morphology of these aggregates, investigated by SEM spectroscopy, showed that the solvent polarity influenced their structures.

1. Introduction

Aggregation of small organic molecules to form large clusters is of large interest in chemistry, physics and biology. In nature, particularly in living systems, self-association of molecules plays a very important role; an example is given by molecular aggregates of chlorophyll that have been found to mediate the primary light harvesting and charge-transfer processes in photosynthetic complexes [1,2]. Molecular aggregates of several dyes have been studied as organic photoconductors [3], as markers for biological and artificial membrane systems [4], as materials with high non-linear optical properties suitable for optic devices [5–8]. Some properties of molecular structure of aggregates permit their use in superconductivity, and other processes [9–11].

An increasing interest in recent years is due to supramolecular assemblies of π-conjugated systems for their potential applications in optoelectronic and photovoltaic devices [12]. Recently, porphyrin assembly has been used for light-driven energy transduction systems, copying the photophysical processes of photosynthetic organisms [13–17].

The porphyrins are a class of natural macrocyclic dyes that play a very important role in the metabolism of living organisms and in electron transport in biological systems, and for these reasons, numerous studies have been carried out for their characterizations [18]. They have played an important role in medicine for their efficacy in photodynamic therapy (PDT) [19] and some porphyrins and their complexes with paramagnetic metals have been used as potential contrast agents [20].

The aggregation and dimerization of porphyrins and metalloporphyrins in aqueous solution have been widely investigated [21,22] and it has been deduced that it is strictly dependent on the chemical physical characteristics, such as, ionic strength and pH; the combination of these factors can facilitate the aggregation processes [23]. The aggregation of porphyrins, changing their spectral and energetic characteristics, influences their efficacy in several applications thus, it is very important take on informations about the dynamics of their aggregation. They react with many metal ions to form easily complexes, and it has been observed that the efficiency of these reactions is affected by their aggregation [24]. Several authors have observed that in the photogeneration of H_2O_2 by porphyrins, the efficiency of production was highly dependent on their aggregation state [25]. Because the aggregates of porphyrins show different characteristics with peculiar spectroscopic properties, the molecular associations of porphyrins were generally investigated using UV–vis absorption and fluorescence spectroscopy [26]. The characteristic of porphyrin molecule with 22 π-electrons causes a strong π–π interaction [27], facilitating the formation of two structure types: "H-type" with bathochromic shift of B and Q bands and "J-type" with blue shift of B band and red-shift of Q band, with respect to those of monomer. The J-type aggregates (side-by-side) were formed for transitions polarized parallel to the long axis of the aggregate, while H-type (face-to-face) for transitions polarized perpendicular to it. Among the numerous porphyrins studied, Coproporphyrin-I (3,8,13,18-tetramethyl-21H,23H-porphine-2,7,12,17-tetrapropionic acid or CPI) is a natural anionic porphyrin and for this reason the knowledge of its chemical properties is very important [28]. In our

* Corresponding author.
E-mail address: rita.giovannetti@unicam.it (R. Giovannetti).

1010-6030/$ – see front matter © 2010 Elsevier B.V. All rights reserved.
doi:10.1016/j.jphotochem.2010.02.003

laboratory several equilibriums and kinetic studies concerning the reactions of CPI with many metal ions were carried out [29,30].

Some studies have demonstrated the phototoxicity of CPI and ZnCPI and that these compounds can be used successfully as a novel photodynamic therapy [31,32]. Amphiphilic carboxylic porphyrins as CPI are selective molecules for tumors based on pH effects [33]; in fact, the increase of anaerobic metabolism of glucose in hyperproliferating tissues leads to lactic acid excretion with consequent acidification that induced the neutralization of carboxylic chains with consequent aggregation that contribute to the retention of this molecule by tumors [34–36].

In this work, with known importance of CPI, we have performed a study on spectral characterization of the aggregate forms of CPI and on the dimerization equilibria in different conditions for acid, salts and hydrogen peroxide addition. The polymerization kinetics have been studied and the aggregate structures were characterized by scanning electron microscopy.

2. Experimental

2.1. Materials

All chemicals (Sigma–Aldrich) were of analytical grade and used without further purification. All the solutions were prepared with Milli-Q water. Stock solution of CPI 4.18×10^{-4} mol l^{-1} was prepared by dissolving 76.1 mg of CPI–dihydrochloride in 500 ml of 0.61×10^{-4} mol l^{-1} sodium hydroxide solution.

2.2. Methods

All the reactions were studied and monitored in the dark, because of the photosensitivity of CPI [37], by a Hewlett-Packard 8452A diode array spectrophotometer with a 1-cm quartz cell well-stoppered and connected to Lauda K2R thermostat. A Metrohm 655 pH meter with a combined electrode (Inlab 413) was used for pH determination.

CPI aggregates for microscopy were prepared by adding to 9.68×10^{-5} mol l^{-1} of CPI, 0.24 mol l^{-1} HCl or 4.41 mol l^{-1} H_2O_2; after 24 h, the liquid phase will be removed. All the samples for scanning microscopy were prepared by drying in vacuum oven at 37 °C, 3–5 μl of the polymeric solution on aluminum stabs using self-adhesive carbon conductive tabs. The samples were sputter coated with carbon by Balzers Med 010 to prevent charging when analyzed by the electron beam. Images of CPI aggregates were obtained with a Leika Cambridge Stereoscan 360 scanning electron microscopy (SEM). Measurements were carried out at an accelerating voltage of 20 kV.

3. Results and discussion

3.1. pH effect on the electronic absorption spectrum

Porphyrins are known to self-associate depending on pH since the protonation reduced the charge and promoted their association. CPI can be considered as an amphiphilic molecule due to the presence of hydrophobic porphine core and of four hydrophilic propionate groups [38].

To obtain information about the aggregation of CPI in aqueous solutions, their forms were characterized studying the pH dependence by spectrophotometric measurements. The CPI is a tetra-anionic porphyrin for the presence of four propionic groups and the possible protonation sites were pyrrole nitrogens and carboxylic groups. In aqueous solution, two or more chemical forms of CPI may exist in equilibrium, depending upon the pH of the solution, that can be characterized from the change of the electronic absorption spectrum. At pH ≥ 10, the CPI exists in the unprotonated form with total charge 4^- and its solution is deep pink colour. The spectrum is characterized by an intense Soret band (B band) in the high energy region at 392 nm with $\varepsilon = (1.782 \pm 0.014) \times 10^5$ M^{-1} cm^{-1} and other four weaker Q bands at 500(IV), 536(III), 556(II) and 606(I) nm (Fig. 1a); because the relative intensities of these bands are such that IV > III > II > I, this spectrum is said to be *etio-type* [39]. The band at 392 nm was previously assigned to be *basic monomer* [40].

On adding HCl to CPI solution up to pH of about 6 (Fig. 1b), solution colour changed to pale pink corresponding to the variation of absorption pattern with a blue shift of the Soret band to 370 nm with $\varepsilon = (1.236 \pm 0.022) \times 10^5$ M^{-1} cm^{-1}; the four Q bands changed the relative intensities in the order (II) > (III) > (IV) > (I). This indicated *H*-dimerization according to the exciton coupling model of Kasha [41–45]; this theory established that the blue shift relative to the monomer band corresponds to linear aggregation dipoles par-

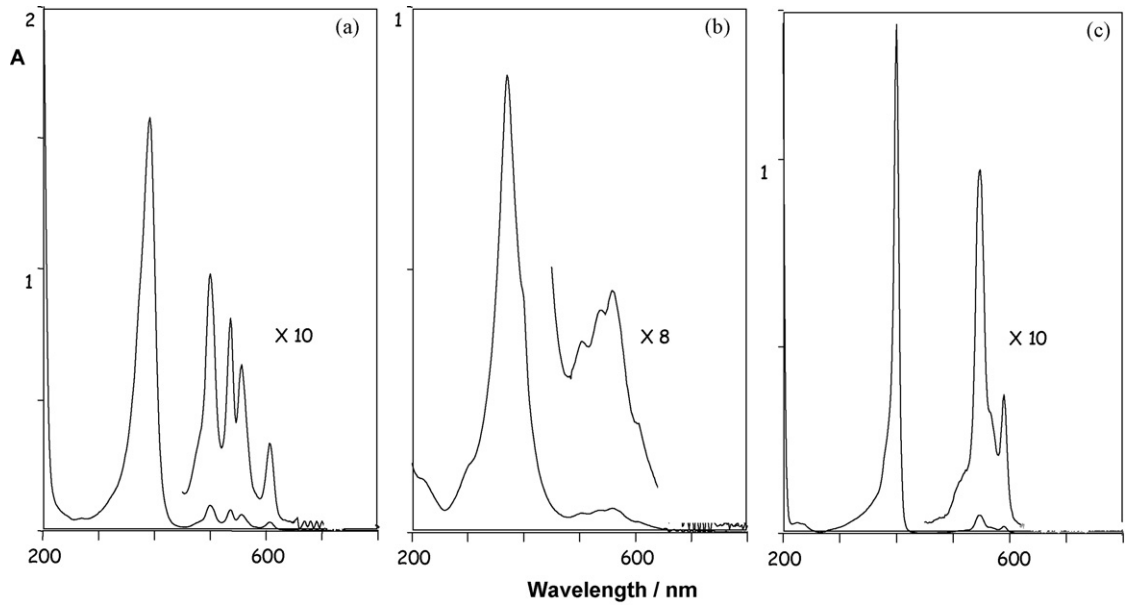

Fig. 1. UV–vis absorption spectra: (a) CPI 7.74×10^{-6} mol l^{-1}, pH 10 (NaOH 3.92×10^{-3} mol l^{-1}); (b) CPI 9.68×10^{-6} mol l^{-1}, pH 6.2 (HCl 1.22×10^{-4} mol l^{-1}, NaOH 3.30×10^{-5} mol l^{-1}); (c) CPI 2.90×10^{-6} mol l^{-1}, pH 1 (HCl 0.122 mol l^{-1}).

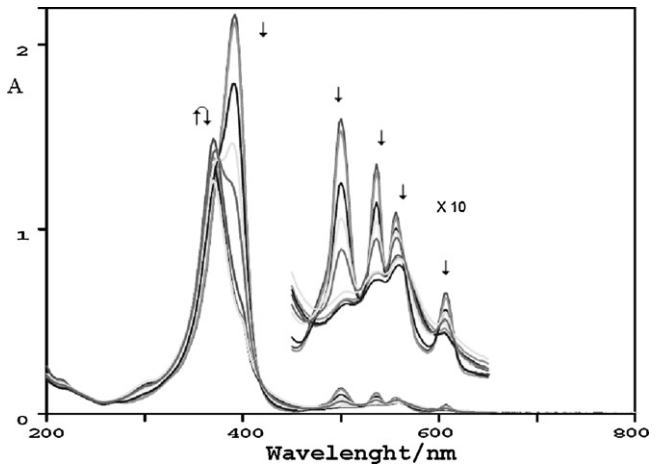

Fig. 2. Change of absorption spectra for 1.21×10^{-5} mol l^{-1} of CPI with pH from 7.22 to 4.46 (HCl concentrations from 4.90 to 18.39×10^{-5} mol l^{-1}).

allel to each other and ordered perpendicularly. The neutral form obtained by the protonation of carboxylic groups favour therefore the formation of *H-dimer* with face-to-face stacking [46].

At pH lower than 4.30 the CPI solution became slightly turbid, and the Soret band intensity decreased markedly, showing highly aggregated form soluble at pH ≤ 1.

At very low pHs (≤1), the protonation of two central nitrogens produced a simplification of the Q band spectrum that collapsed to two bands at 548 and 590 nm while the Soret band showed an intense peak at 400 nm with $\varepsilon = (4.094 \pm 0.090) \times 10^5$ M^{-1} cm^{-1}. This caused a colour change of the solution to bright pink. At this pH because two inner nitrogen atoms were protonated, the total charge is 2$^+$, so another type of monomer CPI (*N-protonated monomer*) was obtained (Fig. 1c).

In the pH range of 7.22–4.46, the changes in CPI absorption spectrum as reported in Fig. 2 are as follows: the band at 392 nm decreased and a new band at 370 nm increased, while in the pH range 7.22–11 an increase of the band at 392 nm of CPI was observed. The isosbestic points at 378 and 420 nm indicated the presence of only two absorbing species in the pH range of 4.46–11.

Fig. 3 shows the s-shape curve of the absorbance at 392 nm versus pH that presents three zones; in the first at pH < 6.28 and in the third, at pH > 7.22, the pH did not influence the absorbances. In the pH range 6.28–7.22 a large change in the absorbance for the CPI dimerization was observed. The *dimer* of CPI was present in the first zone while *basic monomer* in the third zone.

The equilibrium of CPI dimerization and the relative K_D constant can be defined as:

$$2PH_6 \overset{K_D}{\longleftrightarrow} (PH_6)_2 \tag{1}$$

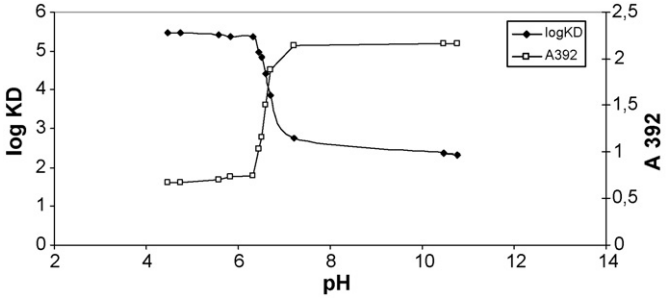

Fig. 3. Changes of the absorbance at 392 nm and log K_D as function of pH for 1.21×10^{-5} mol l^{-1} of CPI.

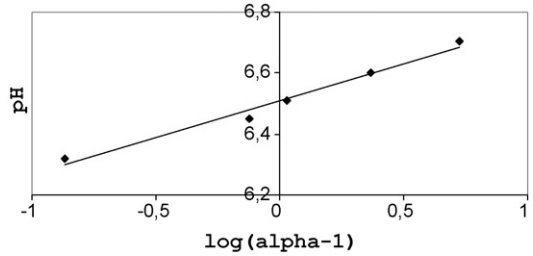

Fig. 4. Correlation of pH with log $(\alpha - 1)$.

$$K_D = \frac{[(PH_6)_2]}{[PH_6]^2} = \left(\frac{\varepsilon_{392}}{2A_{392}^2}\right)(\varepsilon_{392} C_{CPI} - A_{392}) \tag{2}$$

where PH_6 and $(PH_6)_2$ are monomer and dimer CPIs, A_{392} is the absorbance at 392 nm for each pH value and C_{CPI} the analytic concentration of CPI.

The log K_D value has been calculated by absorbance measurements at pH < 5, where only dimeric form of CPI was present and its value is (5.47 ± 0.03) l mol^{-1}. As it may be observed in the graph of Fig. 3, in the range 6–7, the log K_D value is dependent on pH, for the dissociation of the outer propionic groups of porphyrinic ring according to the reaction:

$$(PH_6)_2 \overset{K_a}{\longleftrightarrow} 2PH_{(6-n)}{}^{n-} + nH^+ \tag{3}$$

$$K_a^n = \frac{[PH_{(6-n)}{}^{n-}]^2[H^+]^2}{[(PH_6)_2]} \tag{4}$$

where K_a is the mean acidic constant for a monoprotonation equilibrium; therefore K_D in this pH range must be considered as conditional constant K_D':

$$K_D' = \frac{[(PH_6)_2]}{[PH_6]'^2} \tag{5}$$

where $[PH_6]' = [PH_6] + [PH_{(6-n)}{}^{n-}]$.From the acidic constant, assuming that:

$$\alpha = \frac{K_D}{K_D'\alpha} = \frac{[PH_6]'}{[PH_6]} = \frac{K_a^n + [H^+]^2}{[H^+]^n}$$

$$pH = pK_a + \left(\frac{1}{n}\right)\log(\alpha - 1) \tag{6}$$

The graph of pH against $(1/n)\log(\alpha - 1)$, as reported in Fig. 4, is a straight line where the intercept gives the pK_a value and the slope gives the number of protons in acid–basic equilibrium. The results obtained showed that p$K_a = 6.51 \pm 0.07$ and $n = 4$ therefore the equilibrium (3) may be written as:

$$(PH_6)_2 \overset{K_a}{\longleftrightarrow} 2PH_2^{4-} + 8H^+ \tag{7}$$

This result is fairly in accordance with that obtained previously by fluorescence measurements [40]. Therefore, analyzing the absorption spectra measured at different pHs, the presence of the four CPI forms may be considered: *basic monomer* $PH_2{}^{4-}$ (pH ≥ 10), *H-dimer* $(PH_6)_2$ (6 ≥ pH ≥ 4.3), and *highly aggregated* (4.3 ≥ pH ≥ 1) and *N-protonated monomer* $PH_8{}^{2+}$ (pH ≤ 1).

In order to value the influence of water-soluble co-solvents on the dimerization equilibrium, ethanol or acetonitrile has been added to an aqueous solution of the *H-dimer* $(PH_6)_2$. It has been observed that the effect of the two solvents is similar: *i.e.* the monomeric form of CPI has been observed only when the solvent percentages were greater than 40% and its concentration increased with the solvent percentages. These effects could be attributable only to a change of the solvent that influenced the dimerization equilibria.

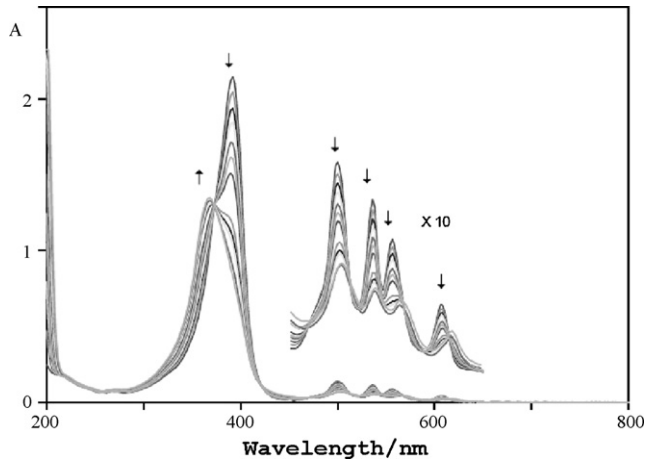

Fig. 5. UV–vis spectral change of CPI 1.21×10^{-5} mol l^{-1} at pH of 6.5 in the presence of NaCl from 0.02 to 2 mol l^{-1}.

3.2. Salt effect

The study of salt effect on the CPI dimerization was carried out at pH 7.22, the pH region where CPI existed in monomeric form ($PH_2{}^{4-}$). The addition of NaCl, KCl, LiCl or $LiNO_3$, at increasing concentrations up to 2 M induced the CPI dimerization for the formation of the "cloud" of counter ions around the CPI molecule that reduced the electrostatic repulsion between the porphyrin molecules. At increasing salt concentrations, the absorption band at 392 nm decreased and a shoulder grew at 370 nm for *H-dimer* formation similar to that obtained by pH decrease. In Fig. 5, the gradual change of the electronic spectrum is showed; it may be observed that in the Q zone the final spectrum showed a small red-shift of the bands I and II. Also in this case the dimer spectrum exhibited an obvious broadening compared with the monomeric implying a 'face-to-face' packing style of the porphyrin molecules [46]. Considering that the *basic monomer* ($PH_2{}^{4-}$) in the presence of alkali–metal salts changed in $(PH_2M_n)^{m-}$ (where M is the cation of the salts) for partial neutralization, the equilibrium of CPI dimerization and the relative K_{DM} constant can be defined as:

$$2(PH_2M_n)^{m-} \overset{K_{DM}}{\longleftrightarrow} (PH_2M_n)_2{}^{2m-} \quad (8)$$

where K_{DM} is:

$$K_{DM} = \frac{[(PH_2M_n)_2{}^{2m-}]}{[(PH_2M_n)^{m-}]^2} = \frac{\alpha_D}{(2C_{CPI}\alpha_M^2)} \quad (9)$$

Table 1
Change of log K_{DM} with several salts at different ionic strengths.

I (mol l^{-1})	log K_{DM}			
	NaCl	KCl	LiCl	$LiNO_3$
0.02	3.86 ± 0.06	4.01 ± 0.07	3.86 ± 0.05	3.94 ± 0.02
0.07	4.37 ± 0.02	4.36 ± 0.02	4.39 ± 0.03	4.49 ± 0.08
0.40	4.89 ± 0.04	4.94 ± 0.05	4.93 ± 0.02	4.96 ± 0.03
2.00	5.26 ± 0.02	5.30 ± 0.03	5.24 ± 0.06	5.30 ± 0.06

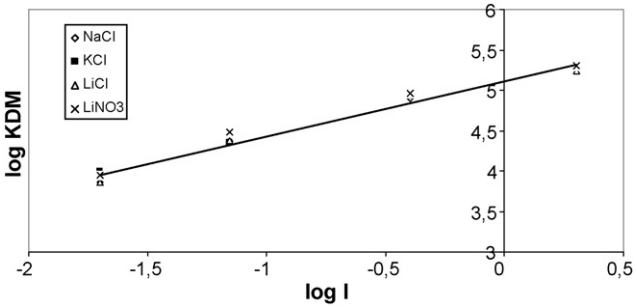

Fig. 6. Log K_{DM} values versus log I in the presence of different salts.

where α_M and α_D were the molar ratios of monomer and dimer respectively and C_{CPI} the analytic concentration of CPI.

The K_{DM} values obtained for each cation at different ionic strengths are reported in Table 1. Dependence of log K_{DM} against log of ionic strength (log I) for different salts is showed in Fig. 6 in which it may be observed that the dimerization depend only on the ionic strength.

3.3. Hydrogen peroxide effect

It is known that CPI, as other porphyrins, photo-generate hydrogen peroxide [25] and the efficiency of this production was strongly dependent on the aggregation of porphyrins; it has been also observed that the dimeric form generally suppressed this formation but no informations exist about the reaction of CPI with hydrogen peroxide.

The addition of H_2O_2 from 0.035 to 7.056 mol l^{-1} into CPI solutions induced pH and spectrum changes in the CPI solutions depending on H_2O_2 concentration; in fact, when CPI is in the monomeric form $PH_2{}^{4-}$, with the addition of H_2O_2, the pH changed from 7.22 to 4.46. While at concentration of H_2O_2 lower than 1.764 mol l^{-1} very small spectral changes of CPI solutions have been observed, at greater concentrations up to 7.056 mol l^{-1}, the acidic

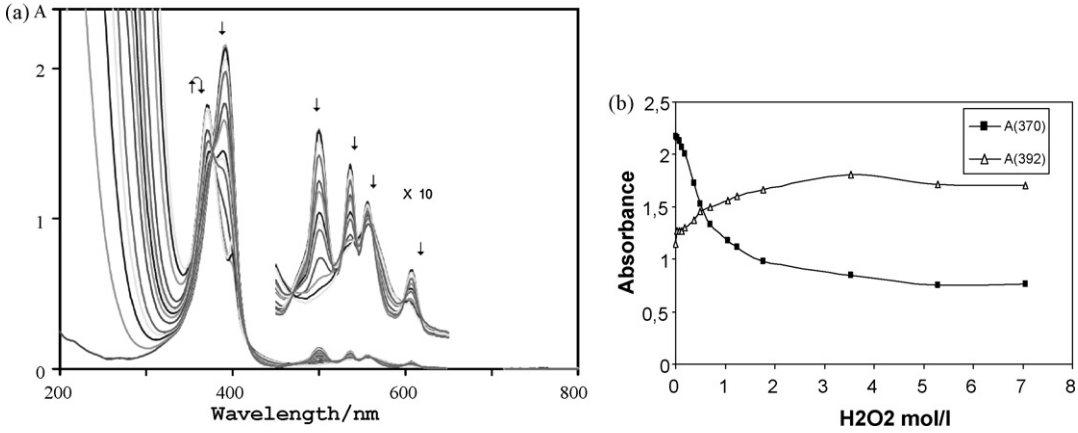

Fig. 7. UV–vis spectral change of CPI 1.21×10^{-5} mol l^{-1} with H_2O_2 from 0.035 to 7.056 mol l^{-1}(pH from 7.42 to 4.20) (a); change of the absorbances at 370 and 392 nm as function of H_2O_2 concentrations (b).

Table 2
Change of $\log K_D$ with pH at different H_2O_2 concentrations.

H_2O_2 (mol l^{-1})	pH	$\log K_D$
0.035	7.42	2.12 ± 0.01
0.106	7.42	3.08 ± 0.04
0.176	7.34	3.43 ± 0.03
0.264	7.16	3.63 ± 0.02
0.529	6.97	4.15 ± 0.07
0.706	6.78	4.41 ± 0.06
0.882	6.61	4.64 ± 0.04
1.058	6.56	4.72 ± 0.07
1.235	6.41	4.89 ± 0.05
1.764	6.20	5.05 ± 0.02
3.528	5.50	5.23 ± 0.08
5.292	4.62	5.36 ± 0.06
7.056	4.20	5.34 ± 0.07

effect induced a similar behaviour as observed for HCl addition: *i.e.* a decrease of absorption band at 392 nm corresponded to an increase of that at 370 nm (Fig. 7). This can be attributed to the formation of *H-dimer*. The dimerization constants (K_D) were obtained by Eq. (2); the values of $\log K_D$ at different pHs, were reported in Table 2 where it may be observed that these reached a constant value at pH lower 5 comparable to that obtained by acidic effect for HCl addition.

Meanwhile, a slow formation of precipitate for CPI polymerization has been observed; the polymeric form obtained in these conditions was soluble at basic pH for the formation of CPI monomeric basic. The polymeric form observed in the H_2O_2 concentration from 1.764 to 7.056 mol l^{-1} corresponded of pH change from 6.20 to 4.46 and therefore at greater pH values with respect to acidic polymerization.

All these results showed that the influence of hydrogen peroxide on the aggregation was different at relatively low or at very high concentrations; this is because while at low concentration a very small effect has been observed on the CPI monomeric form, when the concentration of H_2O_2 is high, the change of solvent and of pH, influenced the dimerization equilibrium.

3.4. Polymerization kinetic

In aqueous solutions of CPI in the pH range from 2.40 to 2.74, the contemporary presence of *N-protonated monomer* PH_8^{2+} (B band at 400 nm) and of *H-dimer* $(PH_6)_2$ (B band at 370 nm) has been observed as reported in Fig. 8; this condition provoked in the time the fast formation of polymeric insoluble form. The

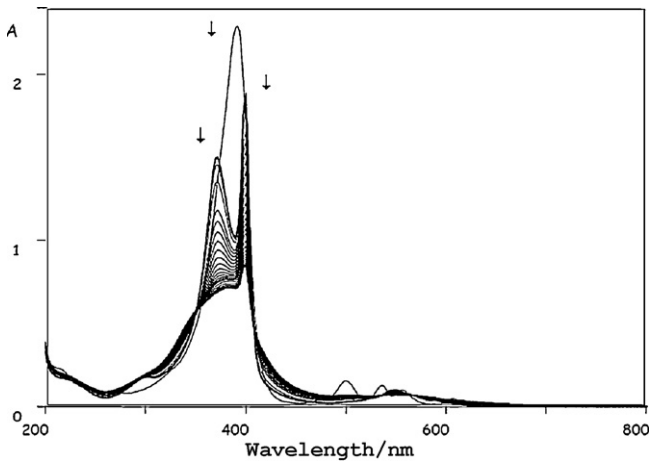

Fig. 8. Time resolved UV–vis spectrum of 1.21×10^{-5} mol l^{-1} of CPI at pH of 2.40.

absorbance changes in the time at 370 nm for different initial pHs showed various speeds of dimeric form disappearance as reported in Fig. 10(I).

The concentrations in the time of *N-protonated monomer* [M] and *dimeric form* [D], calculated from the relative absorbtion maxima at each pH value, showed that the reaction rates were greater according to the initial concentrations of these two species. If k_P is the polymerisation kinetic constant, the reaction rate can be expressed as:

$$v = \frac{-d[M]}{dt} = \frac{-d[D]}{dt} = k_P[M][D] \quad (10)$$

That integrated gives:

$$k_P t = \frac{1}{C_M - C_D} \ln \frac{C_D[M]}{C_M[D]} \quad (11)$$

The plot of the right term of this equation versus t gave good straight lines (Fig. 9 II), the slopes of which represented the values of k_P (C_M and C_D denoted the initial monomer and dimer concentrations). The kinetic constant values for different initial pHs are reported in Table 3. These results showed that the values of $\log k_P$ is linearly dependent of pH in the studied range according to the equation: $\log k_P = -1.93$ pH +2.46 ($R^2 = 0.96$).

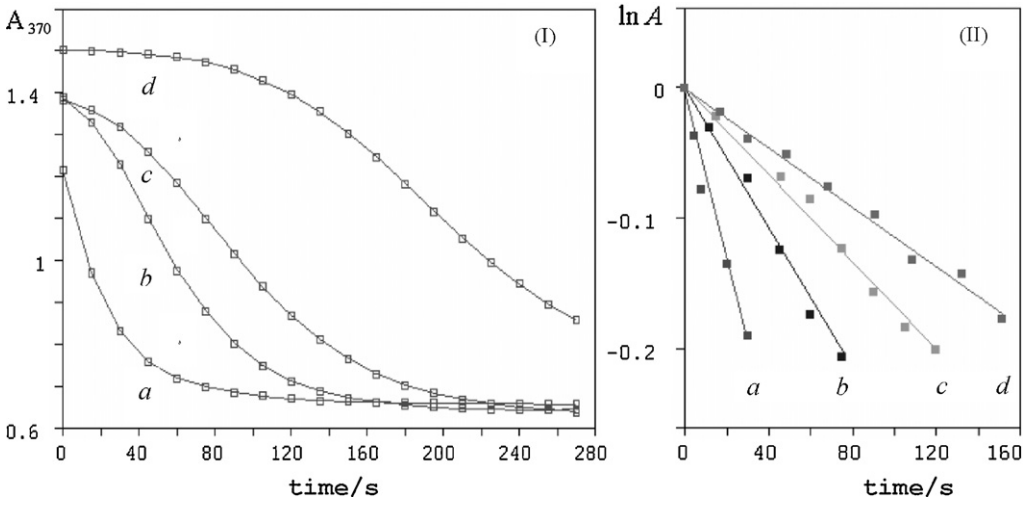

Fig. 9. Changes of the absorbances at 370 nm (I) and $\log A$ (II) in the time for CPI solutions of 1.21×10^{-5} mol l^{-1} at pH: (a) 2.40, (b) 2.57, (c) 2.69, (d) 2.74.

Table 3
Change of $\log k_P$ with pH values.

pH	$\log k_P$
2.40	2.20 ± 0.01
2.57	2.50 ± 0.02
2.69	2.67 ± 0.03
2.74	2.91 ± 0.02

3.5. Morphological characterization of aggregates

To investigate the morphology of the highly aggregate forms of CPI obtained by the addition of HCl and H_2O_2, scanning electron microscopy (SEM) has been used. SEM images of two aggregate types, reported in Fig. 10, showed very different forms. The aggregates obtained with HCl were characterized by regular bipyramidal structures with sizes spanning about from 4 μm × 2 μm up to 10 μm × 5 μm. The aggregate obtained with H_2O_2 showed instead regular fibrous structures with size fibres from 1.5 to 3.0 μm. Two types of aggregates were formed from CPI dimers when the hydrophobic interaction between the molecules is balanced by the charge. As a result of this self-assembly, objects with very different shapes are formed in solution; this is attributable to the different solvophobic interactions among the CPI molecules and HCl or H_2O_2. From these results, it was revealed that this different behaviour depended on the polarity of the solvents: when the solvent is very polar as HCl, the *H-dimers* are further apart and are united in perpendicular way producing more enlarged structures with regular forms.

The less polar H_2O_2 forced instead the *H-dimers* to huddle in perpendicular way producing narrow and linear structures.

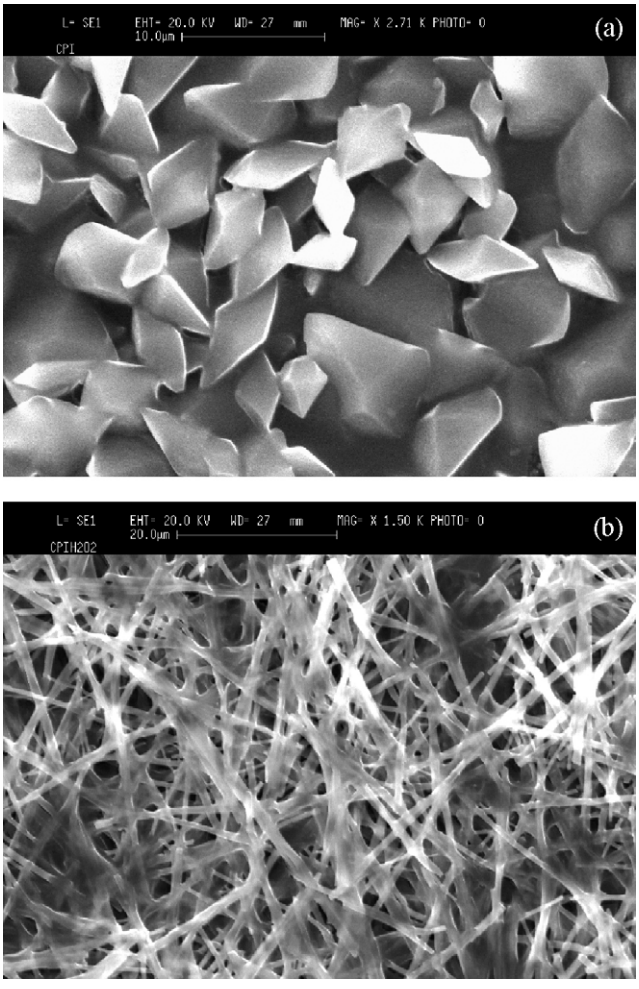

Fig. 10. SEM micrography of aggregates prepared from CPI with (a) HCl; (b) H_2O_2.

4. Conclusions

This study was performed to characterize the pH-dependent ionization and aggregation states of CPI and the results obtained can be of interest to specialists working in the chemical, pharmaceutical, and medical areas. The behaviour of CPI, that presents amphiphilic character due to the presence of hydrophobic porphine core and of four hydrophilic propionate groups, is similar to that of protoporphyrin IX [47]. The UV/vis spectra of CPI aqueous solutions evidenced the presence of different species as a function of pH. At very acidic pH (below 1), the existence of N-protonated monomer for the protonation of propionic groups and of two nitrogen atoms of the CPI core was evident. These results seem in contrast with the behaviour of other water-soluble porphyrins [48–52] that under strong acidic conditions led to the formation of aggregates for the interaction between the opposite charged groups. In the present case, the aggregation could not occur at very acidic conditions for the repulsive effect of the positively charged CPI core. The aggregation of CPI, as that protoporphyrin IX, occurred as a head-to-tail arrangement that minimized the repulsion between the charged groups for the formation of neutral CPI species of *H-dimer*. The dimeric form of CPI has been observed only for slight HCl addition, when ionic strength increased with salt effect or when H_2O_2 was used as prevalent solvent. Monomerization of CPI has been obtained by pH changes and has not been observed for the water-soluble co-solvents addition at percentages lower than 40%; in fact the monomeric CPI form has been obtained only at percentages over than 40% because the change of solvent influenced the dimerization equilibrium.

The SEM morphological study of the CPI aggregates have showed different structures depending of the solvent polarity that forced the *H-dimers* in perpendicular way producing structures narrow and linear or more enlarged with regular forms.

Acknowledgment

The authors would like to express their gratitude to Prof. Vito Bartocci for his very important scientific suggestions.

References

[1] S. Creighton, J. Hwang, A. Warshel, W. Parson, J. Norris, Biochemistry 27 (1988) 774.
[2] W. Kuhlbrandt, Nature 374 (1995) 497.
[3] P. Borsenberger, A. Chowdry, D. Hoesterey, W. Mey, J. Appl. Phys. 44 (1978) 5555.
[4] A. Waggoner, J. Membr. Biol. 27 (1976) 317.
[5] E. Hanamura, Phys. Rev. B 37 (1988) 1273.
[6] F. Sasaki, S. Kobayashi, Appl. Phys. Lett. 63 (1993) 2887.
[7] Y. Wang, Chem. Phys. Lett. 126 (1986) 209.
[8] Y. Wang, J. Opt. Soc. Am. B 8 (1991) 981.
[9] S. Kobayashi, Mol. Cryst. Liq. Cryst. 217 (1992) 77.
[10] P. Schouten, J. Warman, M. De Haas, M. Fox, H. Pan, Nature 353 (1991) 736.
[11] J.P. Collman, J.T. McDeevitt, G.T. Yee, C.R. Leidner, L.G. McCullough, W.A. Little, J.B. Torrance, Proc. Natl. Acad. Sci. U.S.A. 83 (1986) 44581.
[12] A.P.H.J. Schenning, E.W. Meijer, Chem. Commun. (2005) 3245.
[13] M.-S. Choi, T. Aida, I. Yamazaki, T. Yamazaki, Angew. Chem., Int. Ed. 43 (2004) 150.
[14] M.-S. Choi, T. Aida, H. Luo, Y. Araki, O. Ito, Angew. Chem., Int. Ed. 42 (2003) 4060.
[15] M.-S. Choi, T. Aida, I. Yamazaki, T. Yamazaki, Chem. Eur. J. 8 (2002) 2667.
[16] M.-S. Choi, T. Aida, I. Yamazaki, T. Yamazaki, Angew. Chem., Int. Ed. 40 (2001) 194.
[17] H. Luo, M.-S. Choi, Y. Araki, O. Ito, T. Aida, Bull. Chem. Soc. Jpn. 78 (2005) 405.
[18] M. Biesaga, K. Pyrzynska, M. Trojanowicz, Talanta 51 (2000) 209.
[19] R. Bonnett, Chem. Soc. Rev. (1995) 19.
[20] M. Kobayashi, H. Tajiri, T. Hayashi, M. Kuroki, I. Sakata, Cancer Lett. 137 (1999) 83.

[21] I.E. Borissevitch, S.C. Gandini, J. Photochem. Photobiol. B: Biol. 43 (1998) 112.
[22] R.F. Pasternack, E.J. Gibbs, A. Antebi, S. Bassner, L. Depoy, D.H. Turner, A. Williams, F. Laplace, M.H. Lansard, C. Merienne, M. Perrée-Fauvet, J. Am. Chem. Soc. 107 (1985) 8179.
[23] P. Kubat, K. Lang, K. Prochazkovà, P. Anzenbacher Jr., Langmuir 19 (2003) 422.
[24] V.E. Yusmanov, T.T. Tominaga, L.E. Borissevich, H. Imasato, M. Tabak, Magn. Reson. Imaging 14 (1996) 255.
[25] K. Komagoe, T. Katsu, Anal. Sci. 22 (2006) 255.
[26] O. Ohmo, Y. Kaizu, H. Kobayashi, J. Chem. Phys. 99 (1993) 4128.
[27] A.M. Van de Craats, J.M. Warman, Adv. Mater. 12 (2001) 130.
[28] D.L. Lin, L.F. He, Y.Q. Li, Clin. Chem. 50 (2004) 1797.
[29] R. Giovannetti, V. Bartocci, F. Pucciarelli, M. Ricciutelli, Talanta 63 (2004) 857.
[30] R. Giovannetti, V. Bartocci, Talanta 46 (1998) 977.
[31] Y. Sadzuka, F. Iwasaki, I. Sugiyama, K. Horiuchi, T. Hirano, H. Ozawa, N. Kanayama, T. Sonore, Int. J. Pharm. 338 (2007) 306.
[32] Y. Sadzuka, F. Iwasaki, I. Sugiyama, K. Horiuchi, T. Hirano, H. Ozawa, N. Kanayama, N. Oku, Toxicol. Lett. 182 (2008) 110–114.
[33] S. Bonneau, N. Maman, D. Brault, Biochimica et Biophysica Acta 1661 (2004) 87.
[34] D. Brault, C. Vever-Bizet, T. Le Doan, Biochim. Biophys. Acta 857 (1986) 238.
[35] R. Pottier, J.C. Kennedy, J. Photochem. Photobiol., B Biol. 8 (1990) 1.
[36] A.J. Barrett, J.C. Kennedy, R.A. Jones, P. Nadeau, R.H. Pottier, J. Photochem. Photobiol., B Biol. 6 (1990) 309.
[37] R. Giovannetti, V. Bartocci, S. Ferraro, M. Gusteri, P. Passamonti, Talanta 42 (1995) 1913.
[38] J. H. Fuhrhop, J. Koning, In *Membranes and Molecular Assemblies: The Synkinetic Approach*; Stoddart, J. F., Ed.; Monographs in Supramolecular Chemistry; The Royal Society of Chemistry: Cambridge, U.K., 1994.
[39] L.R. Milgrom, The colour of Life, Oxford University Press, 1997.
[40] H. Morales-Rojas, A.K. Yatsimirsky, J. Phys. Org. Chem. 12 (1999) 377.
[41] M. Kasha, M.A. El-Bayoumi, W. Rhodes, J. Chim. Phys. 58 (1961) 916.
[42] R.M. Hochstrasser, M. Kasha, Photochem. Photobiol. 3 (1964) 317.
[43] M. Kasha, Radiat. Res. 20 (1963) 55.
[44] McRae, E. G.; Kasha, M. In Physical Processes in Radiation Biology; Augenstein, L., Mason, R., Rosenberg, B., Eds.; Academic Press: New York, 1964; pp 23-42.
[45] E.G. McRae, M.J. Kasha, Chem. Phys. 28 (1958) 721.
[46] D.M. Chen, Y.H. Zhang, T.J. He, F.C. Liu, Spectrochim. Acta A 58 (2002) 2291.
[47] L.M. Scolaro, M. Castriciano, A. Romeo, S. Patane, E. Cefalì, M. Allegroni, J. Phys. Chem. B 106 (2002) 2453.
[48] D.L. Akins, H.-R. Zhu, C.J. Guo, Phys. Chem. 100 (1996) 5420.
[49] O. Ohno, Y. Kaizu, H.J. Kobayashi, Chem. Phys. 99 (1993) 4128.
[50] J.M. Ribo', J. Crusats, J.A. Farrera, M.L. Valero, J. Chem. Soc., Chem. Commun. (1994) 681.
[51] N.C. Maiti, M. Ravikanth, S. Mazumdar, N.J. Periasamy, Phys. Chem. 99 (1995) 17192.
[52] R. Rubires, J. Crusats, Z. El-Hachemi, T. Jaramillo, M. Lopez, E. Valls, J.A. Farrera, J.M. Ribo, New J. Chem. (1999) 189.